X-ray diffraction by CeB_6

2002 J. Phys.: Condens. Matter 14 4415

(http://iopscience.iop.org/0953-8984/14/17/314)

INSTITUTE OF PHYSICS PUBLISHING JOURNAL OF PHYSICS: CONDENSED MATTER

J. Phys.: Condens. Matter **14** (2002) 4415–4423 PII: S0953-8984(02)34052-9

X-ray diffraction by CeB_6

Stephen W Lovesey

ISIS Facility, Rutherford Appleton Laboratory, Oxfordshire OX11 0QX, UK

Received 20 February 2002, in final form 18 March 2002
Published 18 April 2002
Online at stacks.iop.org/JPhysCM/14/4415

Abstract

Recent x-ray diffraction experiments on CeB_6 held at temperatures below $T_Q \sim 3.2$ K are shown to be fully consistent with properties expected of phase II that arises in the interval of temperature between T_Q and $T_N \sim 2.4$ K. Thomson scattering at reflections $(h/2,\ k/2,\ l/2)$ with odd-integer Miller indices is successfully interpreted on the basis of a distorted CsCl-type structure which supports an antiferro-configuration of Γ_5-type Ce quadrupole moments. Applied to resonant scattering at Ce L_2 and L_3 absorption edges the model also agrees with available data. Intensities calculated as a function of the azimuthal angle show a wealth of strong features which are attributed to the crystal physics of Ce ions in the low-symmetry structure.

1. Introduction

The monovalent metal CeB_6 (cerium hexaboride) is an interesting example of a dense Kondo compound with a simple local f-electron state, and its physical properties have been extensively studied with a variety of experimental techniques. Two recent developments have refreshed the interest in CeB_6. First, NMR [1, 2] and neutron diffraction [3] data gathered in phase II ($T_N < T < T_Q$) have been reconciled, by showing that the Ce quadrupole–quadrupole and octupole–octupole interactions are similar in magnitude [4]. Secondly, x-ray diffraction experiments have been performed [5, 6] with a view to improving our knowledge of the charge distribution in phase II, which is believed to support an antiferro-configuration of Ce quadrupoles [4].

Cerium hexaboride at room temperature crystallizes in a CsCl-type structure (space group $Pm\bar{3}m$, no 221) in which boron octahedra replace Cl ions. In this structure, Ce ions occupy sites with symmetry O_h and there is no ordering of quadrupoles. Evidence of a lower symmetry at Ce sites, and a different space group, comes from the observation [7] at low temperature of $J + 1/2 = 3$ levels in the Ce crystal potential, for Kramers ions with a cubic environment are not expected to obey this rule. More direct evidence is the observation [6] of Thomson scattering in phase II at $(h/2, k/2, l/2)$, where h, k and l are odd integers, which are reflections not indexed by the space group 221. The intensity of the Bragg reflection $(5/2, 3/2, 3/2)$ as a function of temperature is observed to increase below $T_Q = 3.19$ K, which indicates that it is an order parameter of a structural phase transition at T_Q. Additionally, resonance enhancement

of $(h/2,\ k/2,\ l/2)$ intensities is observed [5, 6] as the primary x-ray energy is varied in the immediate vicinity of Ce L_2 and L_3 absorption edges.

We report a first interpretation of the available x-ray diffraction data and look at possible future experiments [6] that can have a significant impact on our knowledge of the structural and magnetic properties of CeB_6. The x-ray diffraction data are found to be consistent with a reduction of symmetry at T_Q, compatible with changes in B_6 octahedra which preserve a cubic Ce lattice. A minimal structure allows two types of octahedron, and if they are nearest neighbours they form two interpenetrating face-centred cubic lattices displaced by a cell edge. Ce ions occupy sites with orthorhombic symmetry and an ordering of Ce quadrupoles is allowed. Use of the two-sublattice model to describe phase II is a working hypothesis which is supported by experimental data. Various mechanisms for the lattice distortion that sets in at T_Q have been discussed [7].

Sections 2 and 3 report our findings for nonresonant and resonant x-ray diffraction based on the distorted CsCl-type structure. Additional details on the calculations are relegated to an appendix. Conclusions are gathered in section 4.

2. Nonresonant diffraction

The amplitude of Thomson scattering is proportional to the overlap of the polarization vectors for the primary ($\boldsymbol{\varepsilon}$) and secondary ($\boldsymbol{\varepsilon}'$) beams of x-rays. The amplitude in question is $\boldsymbol{\varepsilon}\cdot\boldsymbol{\varepsilon}' F_c(\boldsymbol{k})$, where the charge structure factor of an ion,

$$F_c(\boldsymbol{k}) = \left\langle \sum_j \exp(\mathrm{i}\boldsymbol{k}\cdot\boldsymbol{R}_j) \right\rangle, \tag{2.1}$$

and $\boldsymbol{k} = \boldsymbol{q} - \boldsymbol{q}'$ is the change on scattering in the wavevectors. Angular brackets in (2.1) denote a thermal or, equivalently, a time average of the enclosed quantity, and the sum on j is over all electrons in the ion. In the exponential the dependences on $\hat{\boldsymbol{k}} = \boldsymbol{k}/k$ and electron orientation $\hat{\boldsymbol{R}}_j$ are separated by application of a standard identity [8] that employs spherical Bessel functions $j_K(kR)$ and spherical harmonics $Y_q^K(\hat{\boldsymbol{k}})$ and $Y_q^K(\hat{\boldsymbol{R}}_j)$. One finds

$$F_c(\boldsymbol{k}) = (4\pi)^{1/2} \sum_{Kq} \langle j_K \rangle Y_q^K(\hat{\boldsymbol{k}})^* \langle T_q^K \rangle_c, \tag{2.2}$$

where $\langle j_K \rangle$ is the Bessel function transform of the electron radial density. The atomic tensor for charge scattering $\langle T_q^K \rangle_c = \mathrm{i}^K (4\pi)^{1/2} \sum_j \langle Y_q^K(\hat{\boldsymbol{R}}_j) \rangle$. When the unit cell contains several ions, at positions $\{\boldsymbol{d}\}$, the corresponding structure factor is derived from (2.2) by substituting for $\langle T_q^K \rangle_c$ the quantity

$$\Psi_q^K = \sum_{\boldsymbol{d}} \exp(\mathrm{i}\boldsymbol{k}\cdot\boldsymbol{d}) \langle T_q^K \rangle_{c,\boldsymbol{d}}. \tag{2.3}$$

For phase II we adopt a chemical structure, described in the introduction, which contains two sublattices of B_6 octahedra and Ce ions at sites on a cubic lattice with orthorhombic symmetry. The distorted structure is compatible with space group $Fmmm(69)$ with Ce ions at sites $8(f)$ and a point-group symmetry 222 (D_2). The phase transition that reduces space group 221 to space group 69 is not allowed to be continuous in Landau and renormalization group theories [9]. In our model calculation we assume that distortions of B_6 octahedra are extremely small. This, coupled with weak scattering by a B ion, leads to a negligible contribution from B ions at Bragg reflections of interest.

With our model of CeB_6, diffraction at $\boldsymbol{k} = (h/2, k/2, l/2)$ is described by

$$\Psi_q^K = \{1 + (-1)^q\}\{1 - \mathrm{e}^{\mathrm{i}\pi q/2}\}\{\langle T_q^K \rangle_c - (-1)^K \langle T_{-q}^K \rangle_c\}. \tag{2.4}$$

In arriving at (2.4) we have used operations that relate Ce ions in a cell of the two-sublattice model. These operations [10] include reflection in planes normal to the x and y axes, namely, $\langle T_q^K\rangle \to (-1)^K\langle T_{-q}^K\rangle$ and $\langle T_q^K\rangle \to (-1)^{K+q}\langle T_{-q}^K\rangle$. The other relation is rotation by $\pi/2$ about the z-axis, which merely multiplies $\langle T_q^K\rangle$ by the phase $\exp(\mathrm{i}\pi q/2)$.

The finding $\Psi_{q=0}^K = 0$ means that scattering at $(h/2, k/2, l/2)$ is caused by anisotropy in the Ce charge distribution. The orthorhombic symmetry of Ce ion sites restricts the projection q to even integers [11], and Ψ_q^K can be different from zero for $q = \pm 2, \pm 6, \ldots$. Moreover, the atomic tensor for charge scattering, discussed in the appendix, is zero for the rank K equal to an odd integer and thus $\Psi_{-q}^K = -\Psi_q^K$. Since $\langle T_{-q}^K\rangle = (-1)^q\langle T_q^K\rangle^*$ the allowed $\Psi_q^K = 8\mathrm{Im}\,\langle T_q^K\rangle_c$. These features of Ψ_q^K describe an array of multipoles of even rank that alternate in sign on moving between nearest-neighbour Ce sites. The face-centred cubic arrays of charge multipoles are nicely illustrated by Nakao *et al* [5].

In the application of (2.4) to Ce ions the maximum rank $K = 4$, and the structure factor for Thomson scattering is a linear combination of a quadrupole and a hexadecapole. We find, for $\boldsymbol{k} = (h/2, k/2, l/2)$,

$$F_c(\boldsymbol{k}) = 8\sqrt{30}\hat{k}_x\hat{k}_y\{\langle j_2\rangle\langle T_{+2}^2\rangle'' + \tfrac{1}{2}\sqrt{3}\langle j_4\rangle(7\hat{k}_z^2 - 1)\langle T_{+2}^4\rangle''\} \tag{2.5}$$

where $\langle T_{+2}^2\rangle'' = \mathrm{Im}\,\langle T_{+2}^2\rangle$ etc. The spherical quadrupole tensor can be written in terms of purely real Cartesian components of a rank two tensor,

$$\langle T_{+2}^2\rangle = \frac{1}{\sqrt{6}}\langle T_{xx}^2 - T_{yy}^2 + 2\mathrm{i}T_{xy}^2\rangle, \tag{2.6}$$

with

$$\langle T_{+2}^2\rangle'' = (2/3)^{1/2}\langle T_{xy}^2\rangle. \tag{2.7}$$

There is no unique decomposition of a hexadecapole in terms of Cartesian components of a rank four tensor. In a CsCl-type structure $\langle T_{xy}^2\rangle$ belongs to the irreducible representation Γ_5, whereas in $Fmmm$ it belongs to Γ_3.

On turning to an interpretation of data reported by Yakhou *et al* [6] for $(5/2, 3/2, 3/2)$, $(5/2, 1/2, 1/2)$ and $(7/2, 1/2, 1/2)$, the first thing to note about $F_c(\boldsymbol{k})$ is that the factor $(7\hat{k}_z^2 - 1)$ has opposite signs for $k = l = 3/2$ and $1/2$. The sign difference is a possible explanation of the observation that Thomson intensities at $(5/2, 3/2, 3/2)$, and $(5/2, 1/2, 1/2)$ and $(7/2, 1/2, 1/2)$ differ by a factor of 100.

To go further with an interpretation, we ascribe Thomson scattering in phase II of CeB_6 to the f state of Ce^{3+} (^{6}F), and construct the ground-state Kramers doublet from the Γ_8 quartet. Using the notation adopted by Shiba *et al* [4], we find a ground state consistent with orthorhombic symmetry and a saturation magnetic moment [3] $= 1\mu_B$ is spanned by

$$|\psi\rangle = \frac{1}{\sqrt{2}}\{|+\uparrow\rangle + \mathrm{e}^{\mathrm{i}\delta}|-\uparrow\rangle\}, \qquad |\bar{\psi}\rangle = \frac{1}{\sqrt{2}}\{|+\downarrow\rangle + \mathrm{e}^{-\mathrm{i}\delta}|-\downarrow\rangle\}, \tag{2.8}$$

where δ is an unknown phase angle. (Note that the choice $\delta = \pi/2$ makes $|\psi\rangle$ an eigenfunction of T_{xy}^2.) We then find

$$\langle T_{+2}^2\rangle_c'' = \tfrac{1}{7}(2/5)^{1/2}\sin\delta, \qquad \langle T_{+2}^4\rangle_c'' = (5/\sqrt{3})\langle T_{+2}^2\rangle_c'', \tag{2.9}$$

and the corresponding structure factor for Thomson scattering is

$$F_c(\boldsymbol{k}) = \frac{16\sqrt{3}}{7}\hat{k}_x\hat{k}_y\sin\delta\left\{\langle j_2\rangle + \frac{5}{2}\langle j_4\rangle(7\hat{k}_z^2 - 1)\right\}. \tag{2.10}$$

By way of orientation to magnitudes, $(F_c)^2$ evaluated for the reflection $(5/2, 3/2, 3/2)$ and $\sin\delta = 1$ is estimated [12] to have a value of the order of 6×10^{-5} relative to the intensity of a basic structure reflection at the same $\sin\theta/\lambda$.

Values of $F_c(\boldsymbol{k})$ are consistent with data [6] gathered using π-polarized x-rays of energy $= 5.68$ keV. The factor multiplying the unknown quantity $\sin\delta$ on the right-hand side of (2.10) has the value [12] $0.36(-0.49)$, $0.08(0.06)$ and $0.03(-0.77)$ for reflections $(5/2, 3/2, 3/2)$, $(5/2, 1/2, 1/2)$ and $(7/2, 1/2, 1/2)$, respectively. To find the value which represents the observed intensity one multiplies these figures by the x-ray polarization factor $\boldsymbol{\varepsilon} \cdot \boldsymbol{\varepsilon}' = \cos(2\theta)$ in which θ is the Bragg angle, and its value appears in brackets behind the foregoing estimates of $F_c(\boldsymbol{k})$. The intensity at $(5/2, 3/2, 3/2)$ is by far the largest, in accord with the observation, and this result comes from favourable values of $\cos(2\theta)$ and $F_c(\boldsymbol{k})$. The latter is very small for $(7/2, 1/2, 1/2)$, because of a near cancellation of contributions with $K = 2$ and 4, while for $(5/2, 1/2, 1/2)$ the two factors $\cos(2\theta)$ and $F_c(\boldsymbol{k})$ contrive to give an exceptionally small intensity. The reflection $(5/2, 3/2, 3/2)$ was also measured at a lower x-ray energy $= 5.218$ keV. Changing the energy does not change $F_c(\boldsymbol{k})$ but there is a change in intensity through $\cos(2\theta)$.

Absolute values of atomic tensors are rather uncertain. In addition to a quite major uncertainty arising from a poor knowledge of the Ce crystal potential, Kondo fluctuations and the dynamical Jahn–Teller effect have an influence which is difficult to assess. Thomson scattering experiments can improve our knowledge of these effects because intensities are on an absolute scale, unlike signals from resonance-enhanced diffraction.

Turning to the temperature dependence of nonresonant Bragg diffraction it is noted that with a cubic site for a Ce ion the quadrupole and hexadecapole in $F_c(\boldsymbol{k})$ are zero. With this in mind, our explanation of Thomson scattering appearing at reflections $(h/2, k/2, l/2)$ as the sample temperature is lowered through T_Q is in terms of a structural phase transition, heralded by a reduction in site symmetry and concomitant non-zero values of $\langle T^K_{+2}\rangle''_c$. A simple non-ferroelectric soft-mode phase transition has the same critical exponents as the Ising model and the corresponding exponent $\beta \sim 0.33$ is consistent with data [5, 13]. Nagao and Igarashi [14] give a mean-field treatment ($\beta = 0.5$) of a particular model [4] of CeB_6, and also consider the influence of an external magnetic field. In our model, the diffracted intensity from the distorted crystal arises from a quadrupole, and a hexadecapole whose contribution to scattering can be made small by working at reflections with $(7\hat{k}_z^2 - 1) \sim 0$, e.g. $(7/2, 1/2, 3/2)$. With the sample temperature taken below T_N there is additional intensity, which might be due to diffraction by magnetic moments.

The four amplitudes for diffraction by a magnetic crystal are denoted by G_{st} where s and t, respectively, label states of secondary and primary polarization. In keeping with a conventional notation, σ denotes polarization normal to the plane of scattering and π polarization lies in the plane. Compact expressions for G_{st} are achieved by using four complex partial amplitudes [15] such that

$$\begin{aligned} G_{\sigma'\sigma} &= \langle\beta\rangle + \langle\alpha_3\rangle, \qquad & G_{\pi'\pi} &= \langle\beta\rangle - \langle\alpha_3\rangle, \\ G_{\sigma'\pi} &= \langle\alpha_1\rangle - \mathrm{i}\langle\alpha_2\rangle, \qquad & G_{\pi'\sigma} &= \langle\alpha_1\rangle + \mathrm{i}\langle\alpha_2\rangle. \end{aligned} \tag{2.11}$$

Here, $\langle\alpha_1\rangle$ and $\langle\alpha_2\rangle$ are purely magnetic and vanish if the spin and orbital magnetizations are normal to the plane of scattering. $\langle\alpha_3\rangle$ is a linear combination of charge (F_c) and orbital ($\boldsymbol{F}_l$) structure factors, while $\langle\beta\rangle$ is a linear combination of F_c, $\boldsymbol{F}_l$ and the structure factor for spin magnetism, $\boldsymbol{F}_s$. If the spin and orbital magnetizations lie in the plane of scattering $\langle\alpha_3\rangle$ and $\langle\beta\rangle$ are non-magnetic. With regard to orbital magnetism, the amplitudes are independent of the projection of $\boldsymbol{F}_l$ on the scattering wavevector, $\boldsymbol{k}$.

For moderate values of k, $\boldsymbol{F}_s$ and $\boldsymbol{F}_l$ can be constructed from the spin and orbital magnetic moments, to a good approximation. In the event that scattering is by lanthanide ions with properties adequately described by states taken from one manifold of J-states, $\boldsymbol{F}_s$ and $\boldsymbol{F}_l$ are proportional to the structure factor of the total angular momentum $\boldsymbol{F}_J$, namely, $\boldsymbol{F}_s = (g-1)\boldsymbol{F}_J$

and $\boldsymbol{F}_l = (2-g)\boldsymbol{F}_J/2$ where g is the Landé factor. For general $\boldsymbol{k}$ these limiting forms of the magnetic structure factors might not provide a satisfactory interpretation of data. In particular, the limiting forms of $\boldsymbol{F}_s$ and $\boldsymbol{F}_l$ do not contain any information on octupole moments [4] which are believed to be significant in CeB_6. An approach to such features of magnetic x-ray diffraction is offered by theoretical developments made for magnetic neutron diffraction [16].

3. Resonant diffraction

With the primary x-ray energy tuned to a Ce absorption edge structure factors for resonant diffraction are derived directly from Ψ_q^K, given in (2.4), after replacing $\langle T_q^K \rangle_c$ by the appropriate atomic tensor. Atomic tensors for resonant scattering [17] depend on the quantum numbers for the specific absorption edge, and they are different for E1 (electric dipole) and E2 (electric quadrupole) absorption events. Absorption at the L_2 and L_3 edges makes E1 events sensitive to Ce states with d-like character, and most likely 5d states about which we know very little. E2 events at L_2 and L_3 absorption edges are a direct probe of the 4f valence state. In an E1 (E2) event the maximum rank $K = 2(4)$, and in the absence of long-range magnetic order, or an applied magnetic field, tensors with an odd rank are zero. Thus, E1 enhanced diffraction at $(h/2, k/2, l/2)$ by phase II of CeB_6 is described by one tensor of rank two that we shall denote by $\langle T_q^2 \rangle_{5d}$. Moreover, from properties of Ψ_q^K discussed following (2.4), we know that for our model of CeB_6 only one component of $\langle T_q^2 \rangle_{5d}$ contributes to scattering, namely, the imaginary part of $\langle T_{+2}^2 \rangle_{5d}$.

While it is often the case that E1 events are much more intense than E2 events, at present, there are insufficient data for CeB_6 to be confident that E2 events are not a significant contribution to the diffracted signal. This is an important issue, because E2 events are a direct probe of the 4f valence state, that might be settled by performing azimuthal-angle scans [6] in which the crystal is rotated about the Bragg vector. We also predict that such scans on CeB_6 are very different for unrotated and rotated states of polarization.

Intensities as a function of azimuthal angle ψ derived from the result (2.4) for Ψ_q^K are displayed in figures 1 and 2. In all cases, $\boldsymbol{k} = (5/2, 3/2, 3/2)$ and the origin $\psi = 0$ places $(0, \bar{1}, 1)$ normal to the plane of scattering and parallel to the σ component of polarization. Intensity in scattering channels in which the primary polarization is not rotated is twofold periodic in ψ, and we display results for ψ in the range $0^\circ < \psi < 180^\circ$.

In the case of diffraction enhanced by an E1 event the amplitude is expressed in units of $8\langle T_{+2}^2 \rangle''_{5d}$. By way of an example, the E1 structure factor for $\sigma'\sigma$ is

$$F_{\sigma'\sigma}(\boldsymbol{k}) = -\sin^2\beta \sin(2\gamma), \tag{3.1}$$

where the Euler angles β and γ are determined by

$$\cos\beta = \left(\cos\psi - \frac{5}{\sqrt{43}}\sin\psi\right)\Big/\sqrt{2}, \qquad \cot\gamma = (5 + \sqrt{43}/\tan\psi)/6. \tag{3.2}$$

The coefficients in these equations for β and γ are determined by $\hat{\boldsymbol{k}}$ and the choice of origin. (To illustrate this point, the equations that determine β and γ in (3.1) when $\boldsymbol{k} = (1/2, 1/2, 1/2)$ and $\psi = 0$ finds $(1, 1, \bar{2})$ normal to the scattering plane are $\cos\beta = -(2/3)^{1/2}\cos\psi$ and $\tan(\gamma + \pi/4) = \sqrt{3}\tan\psi$.) The quantity displayed in figure 1 is $|F_{\sigma'\sigma}(\boldsymbol{k})|^2$. Equations for $F_{\pi'\sigma}(\boldsymbol{k})$ and $F_{\pi'\pi}(\boldsymbol{k})$ depend on three Euler angles and the Bragg angles and, in view of their complexity, we do not write them out.

Looking at figure 1 we see that intensities as a function of azimuthal angle are quite different in the three channels of scattering. With the origin set by $(0, \bar{1}, 1)$, one finds at $\psi = 0$ $F_{\sigma'\sigma}(\boldsymbol{k}) = 0$ and approximately equal intensities in the $\pi'\sigma$ and $\pi'\pi$ channels. After adjusting

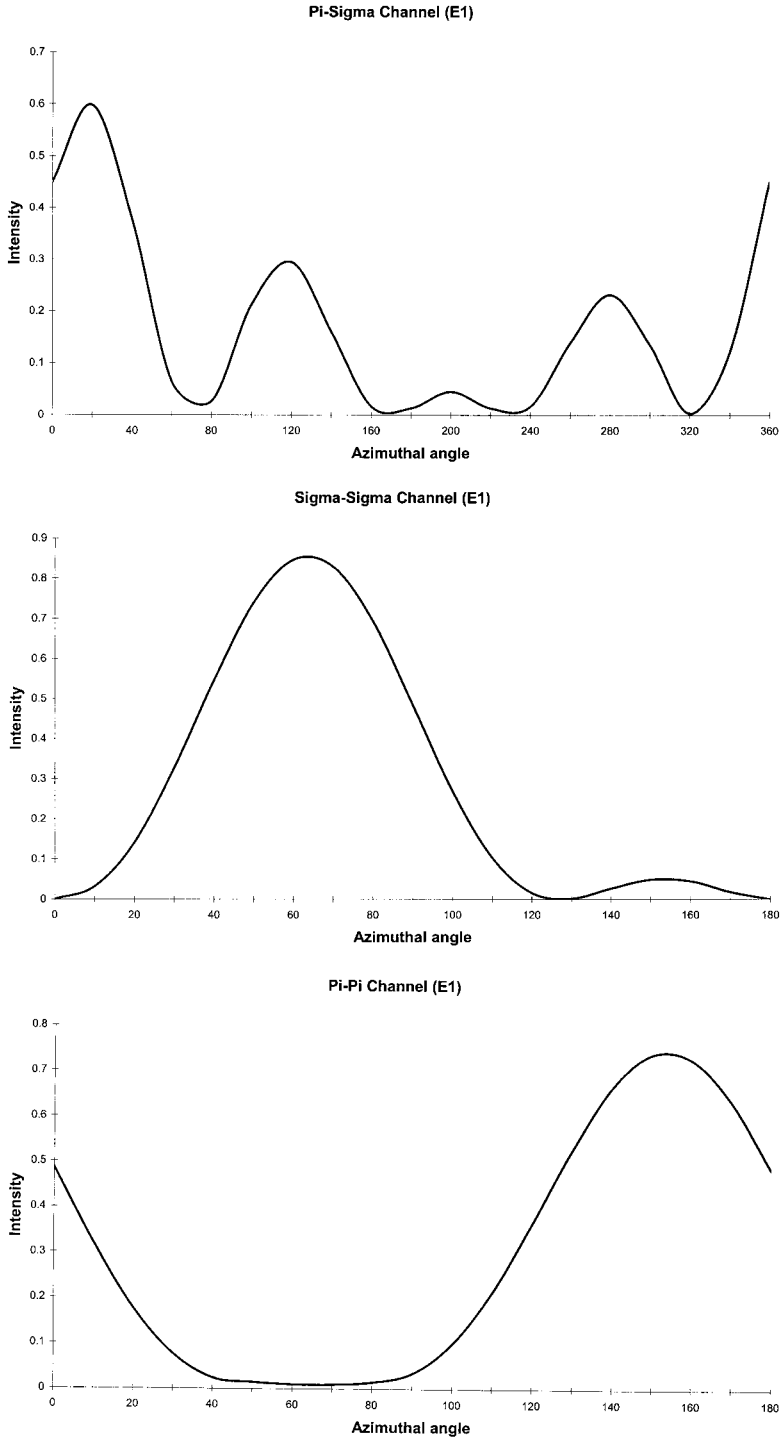

Figure 1. The three panels show intensity at the reflection $(5/2, 3/2, 3/2)$ which is enhanced by an E1 event at the Ce L_3 absorption edge (Bragg angle $\theta = 59.1^\circ$). Intensity in channels of scattering with unrotated polarization is twofold periodic with respect to the azimuthal angle ψ that measures rotation of the crystal around the Bragg wavevector.

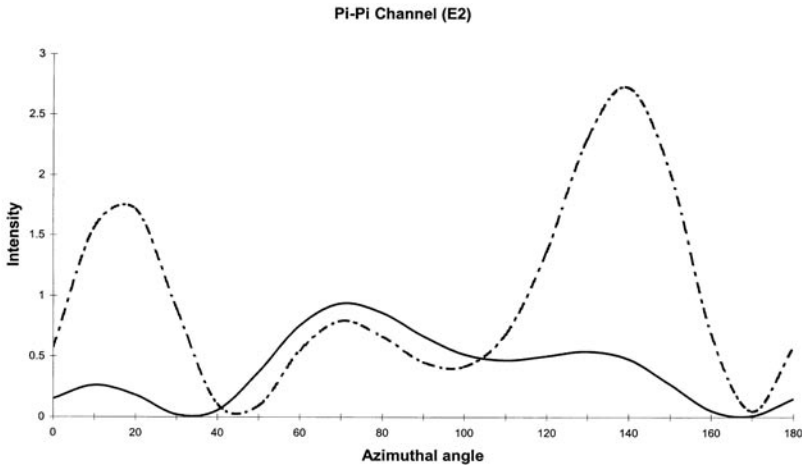

Figure 2. Intensity at $(5/2, 3/2, 3/2)$ in the unrotated π-channel of scattering with intensity enhanced by an E2 event at the Ce L_2 (dashed curve, $\theta = 52.8^\circ$) and L_3 (solid curve, $\theta = 59.1^\circ$) absorption edges. To aid presentation, intensity at the L_2 edge is reduced by a factor of 2.5; the maximum L_2 intensity, at $\psi = 140^\circ$, is six times the L_3 intensity at $\psi = 70^\circ$.

measured intensities for nonresonant diffraction, our findings for $\pi'\sigma$ and $\pi'\pi$ intensities are in accord with observations at the Ce L_3 adsorption edge [6]. Away from $\psi = 0$, maximum intensities in the three channels are about the same but they occur at distinctly different values of ψ. Because the atomic tensor is a common factor in the three structure factors their variation with ψ, and differences between them, is fixed by the crystal physics, namely, the elements of spatial symmetry which enter Ψ_q^K and the direction of the Bragg wavevector relative to crystal axes.

The situation is different for diffraction enhanced by an E2 event because structure factors depend on the ratio of tensors of rank four and two. Using results contained in the appendix we find at the L_2 edge

$$\langle T^4_{+2}\rangle''/\langle T^2_{+2}\rangle'' = 5/\sqrt{3},$$

and at the L_3 edge the ratio is $-16/\sqrt{3}$. The large variation in the ratio is caused by $\langle T^2_{+2}\rangle''$ which is exceptionally small at the Ce L_3 edge; explicit values, (A.8) and (A.9), are derived from the state $|\psi\rangle$ of Ce^{3+} which is given in (2.8). $|F_{\pi'\pi}(\boldsymbol{k})|^2$, as a function of ψ, at the L_2 and L_3 absorption edges is shown in figure 2. Maximum intensities differ by a factor of six, and they occur at different values of the azimuthal angle.

4. Conclusions

We have explored some features in Bragg diffraction patterns from CeB_6 created by a structural transition at T_Q. All observations to hand are consistent with a working hypothesis in which the room-temperature cubic CsCl-type structure (space group 221) distorts to a structure compatible with the space group $Fmmm(69)$. Observed features that are consistent with the hypothesis include: a structual phase transition [6]; Bragg peaks $(h/2, k/2, l/2)$ where Miller indices are odd integers [6]; $J + 1/2 = 3$ energy levels [7] in the Ce crystal potential; Ce quadrupole moments [4,13] with Γ_5-type symmetry; a configuration of quadrupole moments in which moments on nearest-neighbour Ce sites have opposite signs [5]; Thomson intensities [6]

which vary strongly with h, k and l; the resonant enhancement of diffraction at Ce L_2 and L_3 absorption edges [5, 6].

Because structure factors for resonant scattering are very sensitive to properties of the resonant ions which are determined by crystal physics azimuthal angle scans (rotation of the crystal about the Bragg wavevector) are potentially very interesting [6]. With this in mind, we have calculated azimuthal-angle scans on the basis of the successful interpretation of Thomson scattering from CeB_6 held in phase II ($T_N < T < T_Q$). Calculated structure factors, for E1 and E2 events, show a wealth of strong features as functions of the azimuthal angle and the x-ray polarization and beg experimental observation.

While an applied magnetic field causes a significant change in T_Q diffracted intensities will not be much affected, because the structure factor (2.4) is robust with respect to modest magnetic fields. Such fields will only slightly modify atomic tensors of even rank and induce a relatively weak rank-three tensor (octupole).

Acknowledgments

Dr Y Tanaka contributed to initial exploratory work on the nature of x-ray diffraction by CeB_6 while the author was a guest scientist at the RIKEN Harima Institute, Spring-8, at the invitation of Dr K Katsumata. Interpretation of the experimental data and theoretical model has benefited from scrutiny by K S Knight. There has been helpful correspondence and discussion with D A Browne, Z Fisk, J Igarashi, Y Kuramoto, H Shiba and F Yakhou.

Appendix

A matrix element of an arbitrary spherical tensor T^K_q between atomic states $|JM\rangle$ and $|J'M'\rangle$ (for brevity of notation we suppress in these states the quantum numbers S, L, ν etc) is [8]

$$\langle JM|T^K_q|J'M'\rangle = (-1)^{J-M}\begin{pmatrix} J & K & J' \\ -M & q & M' \end{pmatrix}(J\|T(K)\|J') \tag{A.1}$$

where the (purely real) reduced matrix element $(J\|T(K)\|J')$ can depend on all quantum numbers apart from the projections M, q and $M'(M = q + M')$. Using (A.1) one obtains mean values of T^K_{+2} for the state $|\psi\rangle$ of Ce^{3+} which is defined in (2.8):

$$\langle T^2_{+2}\rangle'' = \sin\delta(J\|T(2)\|J)/2\sqrt{210}, \tag{A.2}$$

and

$$\langle T^4_{+2}\rangle''/\langle T^2_{+2}\rangle'' = \frac{10(J\|T(4)\|J)}{3(J\|T(2)\|J)}. \tag{A.3}$$

For Thomson scattering we have introduced a tensor based on a spherical harmonic, namely,

$$\langle T^K_q\rangle_c = \mathrm{i}^K(4\pi)^{1/2}\left\langle\sum_j Y^K_q(\hat{\boldsymbol{R}}_j)\right\rangle. \tag{A.4}$$

Intensity collected at space-group-forbidden reflections is described by projections $q > 0$, and participating charge is in the valence shell. The corresponding reduced matrix element is conveniently expressed in terms of a unit reduced matrix element that depends on all quantum numbers needed to specify the valence shell. Additionally, the charge reduced matrix element contains the one-electron reduced matrix element of a spherical harmonic. We find

$$(J\|T(K)\|J)_c = \mathrm{i}^K\sqrt{8\pi}(l\|Y(K)\|l)W^{(0K)K}, \tag{A.5}$$

and the right-hand side is zero for K an odd integer. In $(l\|Y(K)\|l)$ the maximum K is set by the angular momentum of the one-electron state, l, and $K \leqslant 2l$. The unit atomic matrix element $W^{(0K)K}$ is zero for K larger than $2J$. Results given in (2.9) are derived from (A.2), (A.3) and (A.5).

Turning to matrix elements needed for diffraction enhanced by an E2 event, reduced matrix elements for Ce^{3+} are [17]

$$(J\|T(2)\|J) = \tfrac{2}{49}(\tfrac{6}{5})^{1/2}[-(2\bar{J}+1) \pm \tfrac{31}{9}], \tag{A.6}$$

and

$$(J\|T(4)\|J) = \tfrac{11}{147}(\tfrac{1}{10})^{1/2}[-(2\bar{J}+1) \pm \tfrac{76}{11}]. \tag{A.7}$$

Here $\bar{J} = \frac{1}{2}(\frac{3}{2})$ for the L_2 (L_3) absorption edge and the negative (positive) sign. At the L_2 edge,

$$\langle T^2_{+2}\rangle'' = -\sin\delta/45\sqrt{7}, \tag{A.8}$$

and at the L_3 edge,

$$\langle T^2_{+2}\rangle'' = -\sin\delta/441\sqrt{7}. \tag{A.9}$$

References

[1] Kawakami M *et al* 1981 *J. Phys. Soc. Japan* **50** 432
[2] Takigawa M *et al* 1983 *J. Phys. Soc. Japan* **52** 728
[3] Effantin J M *et al* 1985 *J. Magn. Magn. Mater.* **47/48** 145
[4] Shiba H, Sakai O and Shiina R 1999 *J. Phys. Soc. Japan* **68** 1988
[5] Nakao H *et al* 2001 *J. Phys. Soc. Japan* **70** 1857
[6] Yakhou F *et al* 2001 *Phys. Lett.* A **285** 191
[7] Zirngiebl E *et al* 1984 *Phys. Rev.* B **30** 4052
Terzioglu C *et al* 2001 *Phys. Rev.* B **63** 235110
[8] Edmonds A R 1960 *Angular Momentum in Quantum Mechanics* (Princeton, NJ: Princeton University Press)
[9] Stokes H T and Hatch D M 1988 *Isotropy Subgroups of the 230 Crystallographic Space Groups* (Singapore: World Scientific)
[10] Lovesey S W, Knight K S and Balcar E 2001 *Phys. Rev.* B **64** 054405
[11] Bradley C J and Cracknell A P 1972 *The Mathematical Theory of Symmetry in Solids* (Oxford: Clarendon)
[12] Freeman A J and Desclaux J P 1979 *J. Magn. Magn. Mater.* **12** 11
[13] Yakhou F 2002 private communication
[14] Nagao T and Igarashi J 2001 *J. Phys. Soc. Japan* **70** 2892
[15] Lovesey S W and Collins S P 1996 *X-Ray Scattering and Absorption by Magnetic Materials* (Oxford: Clarendon)
[16] Balcar E and Lovesey S W 1989 *Theory of Magnetic Neutron and Photon Scattering* (Oxford: Clarendon)
[17] Lovesey S W and Balcar E 1997 *J. Phys.: Condens. Matter* **9** 4237
Lovesey S W, Fritz O and Balcar E 1998 *J. Phys.: Condens. Matter* **10** 501